Editors' Suggestion

Nearly fully opened charge density wave gap in the quasi-two-dimensional conductor γ-Mo_4O_{11}: A comparative study with η-Mo_4O_{11}

J. Z. Ke,[1] M. Yang,[1,*] H. P. Zhu,[1] C. Dong,[1] M. Y. Shi,[1] Z. Y. Wu,[1] X. F. Xu,[2] H. K. Zuo,[1] Y. Liu,[3] J. Shi,[3] and J. F. Wang[1,†]

[1]*Wuhan National High Magnetic Field Center & School of Physics, Huazhong University of Science and Technology, Wuhan 430074, China*

[2]*Department of Applied Physics, Zhejiang University of Technology, Hangzhou 310023, China*

[3]*School of Physics and Technology, Wuhan University, Wuhan 430072, China*

(Received 7 September 2021; revised 3 November 2021; accepted 11 November 2021; published 30 November 2021)

Molybdenum bronze η-Mo_4O_{11} with a monoclinic structure has received continued interest due to a variety of magnetotransport properties in its charge density wave (CDW) state, while the orthorhombic phase γ-Mo_4O_{11} has been less reported. We successfully grew high-quality γ-Mo_4O_{11} single crystals via a chemical vapor transport method. Specific heat, magnetic susceptibility, and various electric transport properties in DC and pulsed fields were carefully measured. Our main findings include (1) γ-Mo_4O_{11} belongs to a quasi-two-dimensional (Q2D) system and undergoes a transition at $T_{CDW} = \sim 96$ K due to a CDW instability. Unlike the robust transition in η-Mo_4O_{11}, the CDW modulation in γ-Mo_4O_{11} is rather broad and flexible, which results in negligible anomaly in specific heat. (2) γ-Mo_4O_{11} shows a clear nonlinear current-voltage relation below T_{CDW} due to a sliding motion of the CDW electrons. This indicates that the CDW gap in γ-Mo_4O_{11} is nearly fully opened, and the residual small number of electrons contribute to the CDW transport, different from the situation in η-Mo_4O_{11}. (3) The interlayer magnetoresistivity exhibits magnetic transition at ~5 T and quantum oscillations at $B > 15$ T in applied magnetic fields up to 60 T. These field-induced oscillations featured with two main frequencies ($f_\alpha = 30$ T and $f_\beta = 131$ T) are reminiscent of a Fermi surface reconstruction by magnetic breakdown in a strong field in η-Mo_4O_{11}. In this paper, we reveal that γ-Mo_4O_{11} is distinct from traditional quasi-one-dimensional or Q2D CDW compounds and provide an opportunity to study the CDW electrons and nonlinear transport properties in such a Q2D system.

DOI: 10.1103/PhysRevB.104.195154

I. INTRODUCTION

One common viewpoint related to the low-dimensional purple bronze family is that hidden Fermi surface (FS) nesting gives rise to a charge density wave (CDW) formation that destroys the nested part of the original FSs [1]. Due to an imperfect nesting of the FS, some hole and electron pockets may remain, and the system thus presents many exotic transport properties in its CDW state. For example, the well-studied quasi-two-dimensional (Q2D) purple bronzes $A_{0.9}Mo_6O_{17}$ ($A =$ Na, K, or Tl) are known for their pronounced Shubnikov–de Haas (SdH) oscillations and magnetic breakdown effect below their CDW temperatures [2–5]. Similarly, the quasi-one-dimensional (Q1D) purple bronze $Li_{0.9}Mo_6O_{17}$, which is expected to possess the coexistence of CDW and superconductivity at low temperatures, was widely reported for its possible spin-triplet superconductivity and rare Tomonaga-Luttinger liquid characteristics [6–9].

Another interesting system among the purple bronze family is the two phases of the molybdenum oxide Mo_4O_{11}, monoclinic η and orthorhombic γ. Both η-Mo_4O_{11} and γ-Mo_4O_{11} possess hidden Q1D FS nesting and thus CDW instability at low temperatures. In the two compounds, the FS is partially gapped out due to an imperfect nesting, and the resistivity remains its metallic character in the CDW state. Particularly η-Mo_4O_{11} shows two successive CDW transitions, while γ-Mo_4O_{11} only exhibits one CDW transition [10,11]. Previous high-resolution linear thermal expansion measurements on γ-Mo_4O_{11} exhibited strongly anisotropic behavior and verified that this material should be classified as a Q2D system [12]. On the other hand, according to previous transport and thermoelectric experiments for η-Mo_4O_{11}, ~70% of the original electron band and 78% of the hole band are nested below the first CDW transition temperature T_{CDW1} [13]. With further decreasing temperature, only small pockets (~0.2%) remain at $T < T_{CDW2}$ [13]. In addition, η-Mo_4O_{11} has been the subject of extensive investigations over the past decades for its possibility of bulk quantum Hall effect, rapid quantum oscillations, and an anomalous pressure-induced metal-to-insulator transition [14–18]. Specifically, our recent high-field transport experiments discovered that the magnetoresistivity (MR) of η-Mo_4O_{11} shows complex SdH oscillations and an abrupt structure transition in the second CDW state [19]. As a result, the high-field FS picture of η-Mo_4O_{11} is constructed based on a field-induced FS reconstruction model.

However, in contrast to η-Mo_4O_{11}, the FS structure of γ-Mo_4O_{11} in the low-temperature CDW state has not been revealed in experiment and thus is still an open question. Moreover, reports of the magnetotransport property of γ-Mo_4O_{11} are lacking. Despite the slight difference of structure, the conduction electron concentration, the FS, and the

*Corresponding author: ming_yang@hust.edu.cn

†Corresponding author: jfwang@hust.edu.cn

band structure of the two compounds are expected to be very similar in the normal phase $T > T_{CDW}$ [11]. In this regard, an obvious question is whether the electrons in γ-Mo_4O_{11} could exhibit some intriguing field-induced quantum behaviors as in η-Mo_4O_{11}. Indeed, understanding the evolution of electronic structure in high magnetic fields is important, and the interplay between the magnetic field and the CDW is certainly worthy of study. Especially in the unconventional superconductors, such as the kagome metal AV_3Sb_5 (A = K, Rb, or Cs), the role of the CDW has been intensely investigated for its competition and coexistence with superconductivity [20,21]. The comparative study on the two compounds may offer an opportunity to clarify the related controversies in the CDW and superconductivity fields. Therefore, it is desirable to explore the magnetotransport behavior of γ-Mo_4O_{11} that can reveal its band structure and help us to understand the difference in the CDW-related properties between η-Mo_4O_{11} and γ-Mo_4O_{11}.

We successfully grew γ-Mo_4O_{11} single crystals using a chemical vapor transport (CVT) method and identified their high quality via x-ray diffraction (XRD) and energy dispersive spectroscopy (EDS) measurements. Moreover, comprehensive magnetic, specific heat, and transport measurements on γ-Mo_4O_{11} and η-Mo_4O_{11} single crystals were carried out over a broad temperature range. Several key features associated with CDW instability are uncovered in steady-state fields via a comparative study on γ-Mo_4O_{11} and η-Mo_4O_{11}. Furthermore, we performed a magnetotransport experiment on a high-quality γ-Mo_4O_{11} single crystal by applying a high field. Interestingly, the high-field MR up to 60 T shows quantum oscillations, which provide a platform for us to study its FS structure at low temperatures. In addition, the comparative study of the high-field oscillations supports that γ-Mo_4O_{11} has a nearly fully opened CDW gap and thus requires a higher critical field to observe its highest breakdown frequency in experiment.

II. EXPERIMENTS AND CHARACTERIZATIONS

Single crystals of γ-Mo_4O_{11} were grown by a CVT method in a two-zone furnace. Reagents MoO_2 and MoO_3 were prepared as the starting materials with I_2 as the carrier gas. The specific process was described in the previous paper on the single-crystal growth of η-Mo_4O_{11} [22]. The small difference in the crystal growth for η-Mo_4O_{11} and γ-Mo_4O_{11} is that the high temperature is $T_H = 740\,^\circ$C, and low temperature is $T_L = 680\,^\circ$C for γ-Mo_4O_{11} instead of $T_H = 540\,^\circ$C and $T_L = 510\,^\circ$C for η-Mo_4O_{11}. The single crystals grown via a CVT method were thin plates elongated along the *ab* plane, which are appropriate for the transport measurement. The crystal structure and lattice parameters of the as-grown crystals were examined by the XRD technique. The EDS was measured via an electron probe microanalysis system. The susceptibility measurements were carried out in a 7 T magnetic property measurement system (Quantum Design SQUID-VSM). The current-voltage (I-V) curves and the electrical transport measurements were performed by a 9 T physical property measurement system (PPMS). The specific heat was measured by a relaxation method in the PPMS. The high-field transport experiments were carried out using a pulsed magnet up to 60 T at the Wuhan National High Magnetic Field Center.

Figure 1(a) exhibits the crystal structure of γ-Mo_4O_{11}, which belongs to the orthorhombic space group $Pn2_1a$. The unit cell of γ-Mo_4O_{11} consists of two slabs and is marked by the dotted lines as illustrated in Fig. 1(a). Note that η-Mo_4O_{11} ($\beta = 94.42^\circ$) and γ-Mo_4O_{11} ($\beta = 90^\circ$) have a similar structure and are built with a MoO_4 tetrahedron and a MoO_6 octahedron. The $4d$ conducting electrons are confined in the MoO_6 octahedron layers that are separated from each other by the insulating MoO_4 tetrahedron layers, resulting in a special Q2D electron system. Figure 1(b) displays the collected γ-Mo_4O_{11} samples, which has a clear surface. Figure 1(c) shows the typical XRD pattern of the as-grown crystals. Only the $(00l)$ Bragg peaks can be observed, indicating that the clear surface is the *ab* plane. In addition, the lattice constants are identified to be $a = 6.803(11)$ Å, $b = 5.436(14)$ Å, and $c = 24.310(2)$ Å for the grown samples, also consistent with previous studies [12,23,24]. A characteristic spectrum obtained by EDS is displayed in the inset of Fig. 1(c). Only the peaks of the Mo and O elements are found. All results mentioned above suggest that the grown samples are γ-Mo_4O_{11} featured with a high quality.

III. RESULTS AND DISCUSSION

A. Temperature-dependent CDW transition in γ-Mo_4O_{11}

Figure 2 summarizes the temperature-dependent ρ_b ($I//b$ axis) and ρ_c ($I//c$ axis) of γ-Mo_4O_{11} under 0 T (black lines) and 9 T (red lines), respectively. Overall, the zero-field ρ_b and ρ_c of γ-Mo_4O_{11} show a metallic temperature dependence at high temperatures. With the decrease of temperature, an upturn in resistivity is observed in the vicinity of $T_{CDW} \sim 96$ K since the opening of the CDW gap leads to a significant decrease of the density of states at the Fermi level. Note that the CDW transition in resistivity is rather broad, not a dramatic upturn as those observed in other molybdenum bronzes [3,9,22,25,26]. Below T_{CDW}, the resistivity increases monotonically and tends toward a finite value at the zero-temperature limit, which indicates the gap opening process continues to the lowest measurement temperature in γ-Mo_4O_{11}. The anisotropy of resistivity at 300 K extracted from Fig. 2 is about 1:11 for ρ_b:ρ_c, which well supports the Q2D nature of this compound. In addition, the resistivity under 9 T shows a notably positive MR effect below T_{CDW}, while in the high-temperature range the zero-field resistivity almost coincides with the resistivity under 9 T. For a comparison, we also demonstrate the related data of η-Mo_4O_{11} in this plot, which would be discussed separately in the next part.

The temperature-dependent susceptibility results of γ-Mo_4O_{11} for the $B//c$ axis and the $B//ab$ plane are shown in Fig. 3(a). The susceptibility curves display a phase transition at ~96 K for both field directions, which also can be ascribed to a decrease of the density of states at the Fermi level and can well correspond to the upturn observed in resistivity. Note that the CDW transition in susceptibility is very weak along the *c* axis, while it is notably robust along the *ab* plane. This may suggest that the CDW modulation occurs mainly in the *ab* plane and is relatively weak along the *c* axis. On the other hand, the susceptibility is attributed to a Pauli paramagnetic effect, and the values thus are insignificant in this compound.

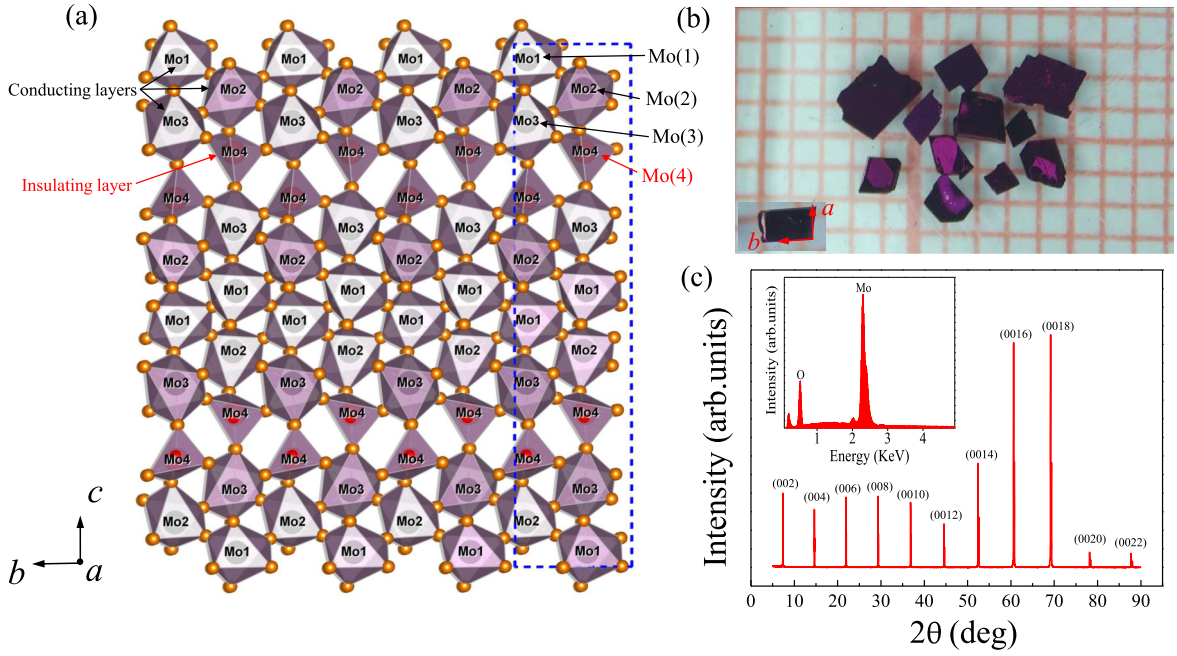

FIG. 1. (a) Crystal structure of γ-Mo_4O_{11}. The blue dotted lines mark a unit cell of γ-Mo_4O_{11}. (b) Collected single crystals, which display a clear surface. The inset of (b) shows the crystallographic directions of the sample. (c) X-ray diffraction (XRD) pattern of γ-Mo_4O_{11} for the (00l) plane. The inset of (c) exhibits a typical energy dispersive spectroscopy (EDS) spectrum.

The CDW instability of γ-Mo_4O_{11} has also been studied by the specific heat measurement using a long-relaxation calorimeter. As shown in Fig. 4, the specific heat curve C_p of γ-Mo_4O_{11} (red line) does not show any anomaly at the CDW transition temperature. This may imply that the CDW instability in γ-Mo_4O_{11} is a second-order phase transition. It is well known that, in the Q1D blue bronze $K_{0.3}MoO_3$, the specific heat shows a very sharp λ phase transition at the CDW temperature accompanied by a strong lattice modulation [27]. On the other hand, in the Q2D purple bronze $K_{0.9}Mo_6O_{17}$, the resistivity displays a notable CDW phase transition [25]. However, the C_p result of $K_{0.9}Mo_6O_{17}$ only shows a broad bump [28]. It is not a typical λ specific heat anomaly like Q1D CDW systems, signaling a relatively weak lattice modulation in Q2D CDW systems. Hence, it is not surprising that, in the Q2D γ-Mo_4O_{11}, we cannot detect a specific heat transition.

A summary of this part: we defined the CDW transition of γ-Mo_4O_{11} at $T_{CDW} \sim 96$ K via the resistivity and magnetic susceptibility measurements. We find the CDW transition in γ-Mo_4O_{11} is relatively flexible and cannot be detected by the specific heat measurement. This may be due to a weak lattice modulation in this Q2D system.

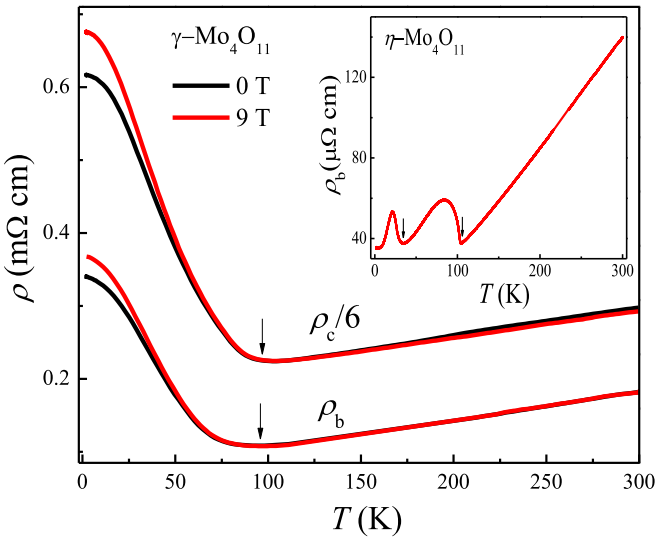

FIG. 2. Temperature-dependent ρ_b and ρ_c of γ-Mo_4O_{11} under 0 T (black lines) and 9 T (red lines), respectively. Black arrow represents the charge density wave (CDW) transition at $T_{CDW} \sim 96$ K. The inset shows the temperature-dependent ρ_b of η-Mo_4O_{11}. Black arrows denote the two CDW transitions at $T_{CDW1} = 105$ K and $T_{CDW2} = 30$ K.

B. The magnetotransport in the CDW state of γ-Mo_4O_{11}

It is well known that the nonlinear I-V transport property appears in the CDW state for the Q1D blue bronzes featured with a fully opened gap, such as $A_{0.3}MoO_3$ (A = K, Rb, or Tl) [29,30]. This nonlinear transport behavior is because of the sliding motion of CDWs in the presence of an applied electric field. However, for the Q2D purple bronzes, the nonlinear behavior in transport has been rarely reported with the exception of $TlMo_6O_{17}$; Tian *et al.* [26] present a nonlinear I-V curve of this compound at 2 K. Nevertheless, strong evidence of such nonlinear transport behavior is still lacking in Q2D systems, probably because the modulation of the CDW is weak, or the huge number of the normal electrons smears the transport of CDW. The reason is unknown at present. However, our results on γ-Mo_4O_{11} clearly demonstrate this nonlinear transport phenomenon in the Q2D CDW system. As

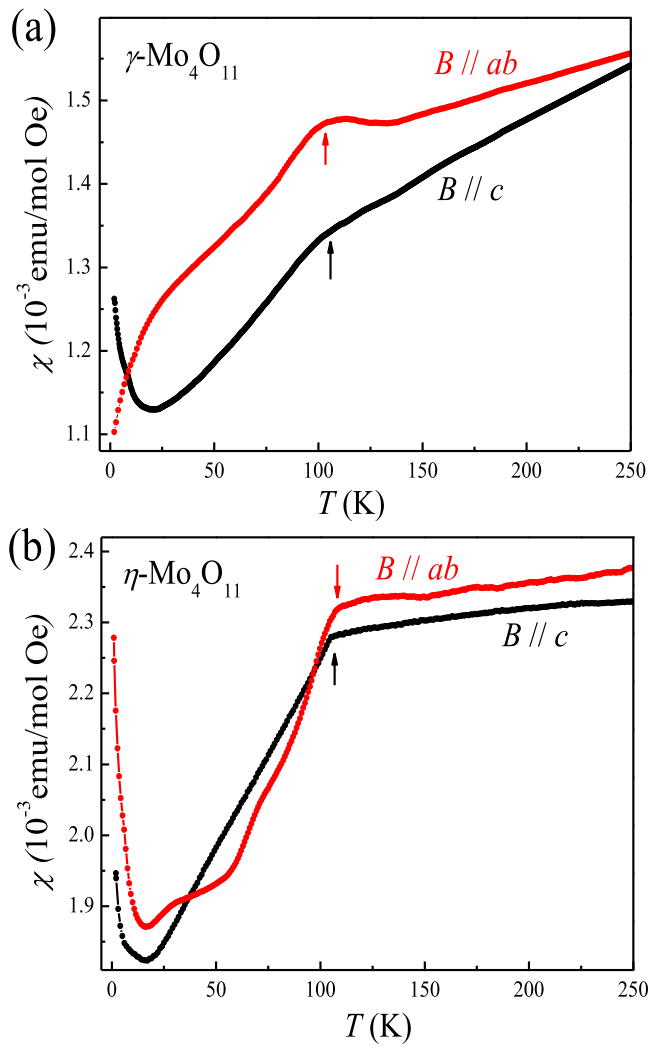

FIG. 3. Temperature-dependent susceptibility measured at $B = 1$ T with the $B//c$ axis and with the $B//ab$ plane for (a) γ-Mo_4O_{11} and (b) η-Mo_4O_{11}. The arrows denote the charge density wave (CDW) transition temperatures at 96 K and 105 K, respectively.

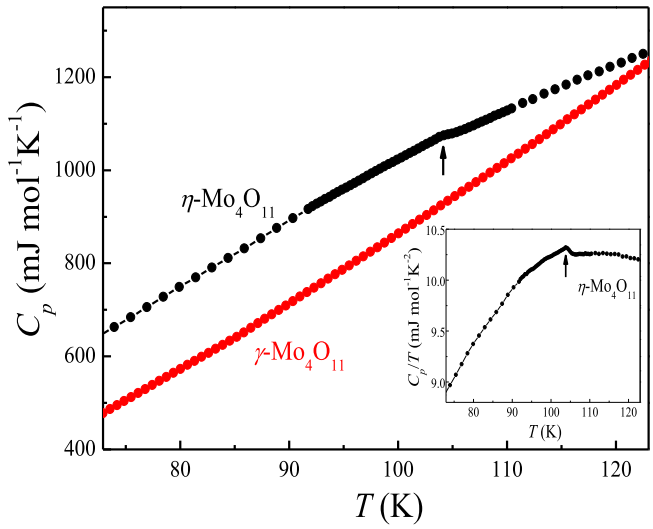

FIG. 4. Temperature-dependent specific heat C_p at zero field for η-Mo_4O_{11} and γ-Mo_4O_{11}, respectively. The inset shows C_p/T of η-Mo_4O_{11} for clarity.

shown in Fig. 5(a), the *I-V* curves of γ-Mo_4O_{11} are exhibited over a broad temperature range. Evidently, a nonlinear *I-V* characteristic is discovered for γ-Mo_4O_{11} below T_{CDW}. With the increase of temperature, the nonlinear transport behavior disappears at $T > 90$ K. These data illustrate clearly how the nonlinear *I-V* relation evolves with the temperature. There is a remarkable deviation of the *I-V* characteristic from linearity above $I = 30$ mA at low temperatures, as denoted by the arrow in Fig. 5(a). This suggests that the CDW gap in γ-Mo_4O_{11} should be nearly fully opened, and the residual small number of electrons contribute to the CDW transport.

To investigate the magnetotransport behavior of γ-Mo_4O_{11}, the MR and Hall resistance were measured using a PPMS up to 9 T. Figure 6(a) shows the magnetic field-dependent ρ_b at various temperatures and with the $B//c$ axis. It is found that ρ_b increases linearly with the field in the measured temperature range. The inset of Fig. 6(a) displays the Hall resistance at $T = 2$ K. The Hall resistance is positive and increases with the field, indicating that the dominating carriers are holes for γ-Mo_4O_{11}. Figure 6(b) shows the magnetic field-dependent ρ_c with the $B//I//c$ axis. Here, ρ_c increases with the field and reaches a maximum at $B \sim 5$ T for $2\,\text{K} < T < 40\,\text{K}$, indicative of a possible field-induced CDW transition. The decreased trend of ρ_c at $B > 5$ T could be connected with a suppression of the CDW order by the magnetic field, which would weaken the CDW gap and lead to an increase of the carrier density [31–33]. As the temperature further increases to 70 K, ρ_c eventually exhibits linear dependence with the field.

In a previous work, Canadell *et al.* [34] studied the band structure of γ-Mo_4O_{11} and mapped the schematic FS in the normal phase ($T > T_{CDW}$) via a tight-binding band calculation. They proposed that there are two electron and hole FS areas occupying equally 25% of the first Brillouin zone S_{BZ} in the normal state of γ-Mo_4O_{11}. However, there is no experimental or theoretical evidence for the FS structure of γ-Mo_4O_{11} in the CDW state so far. Indeed, measurement of the high-field quantum oscillation is an effective approach to study the size and shape of the FS by analyzing the obtained frequency. Furthermore, the high-field technique has been actively utilized in exploring the competing electronic orders in strongly correlated systems over the past years. Hence, to gain more insight into the nature of the electronic state and FS structure, we further conduct high-field MR experiments up to 60 T. Figure 7(a) shows the magnetic field-dependent ρ_c of γ-Mo_4O_{11} at various temperatures from 1.6 to 70 K. Interestingly, ρ_c increases sharply and shows quantum oscillations at $B > 15$ T. With the increase of temperature, the quantum oscillations vanish for $T > 30$ K. In addition, the second derivative curves of ρ_c as a function of B are displayed in Fig. 7(b) to further analyze the FS structure, which exhibits a complex oscillation behavior in a wide field range. The quantum oscillations show different periods, and the amplitude gradually decreases with increasing temperature, which is a typical character of the conventional SdH oscillation. The subsequent fast Fourier transform (FFT) analysis focused on the high-field oscillations was performed. The FFT spectra are

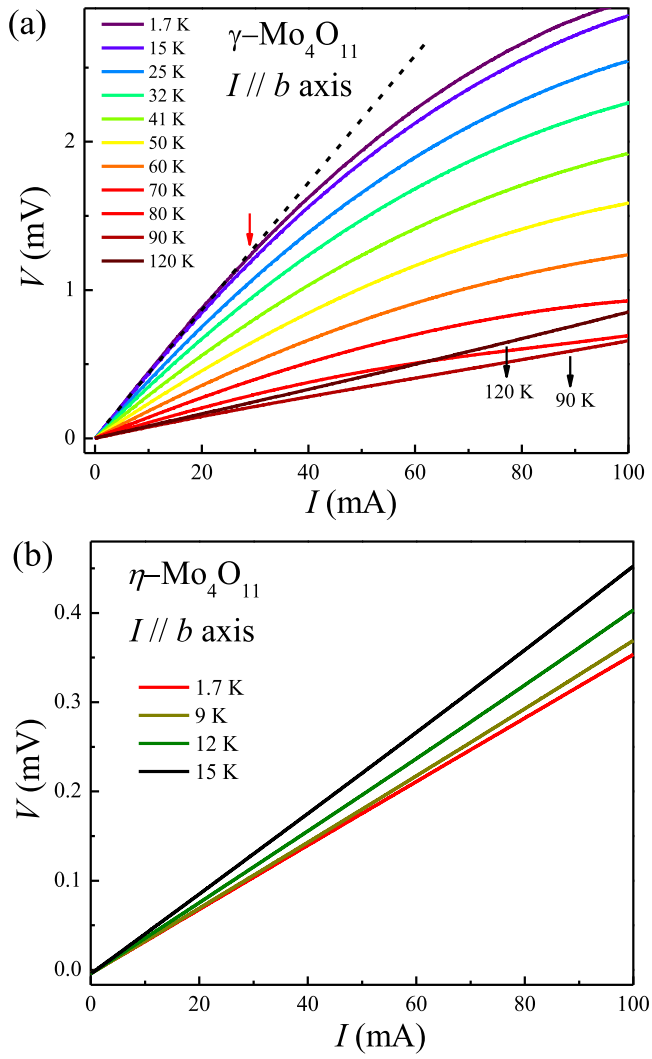

FIG. 5. *I-V* curves of ρ_b at various temperatures for (a) γ-Mo_4O_{11} and (b) η-Mo_4O_{11}. The red arrow in (a) denotes the threshold current for γ-Mo_4O_{11}.

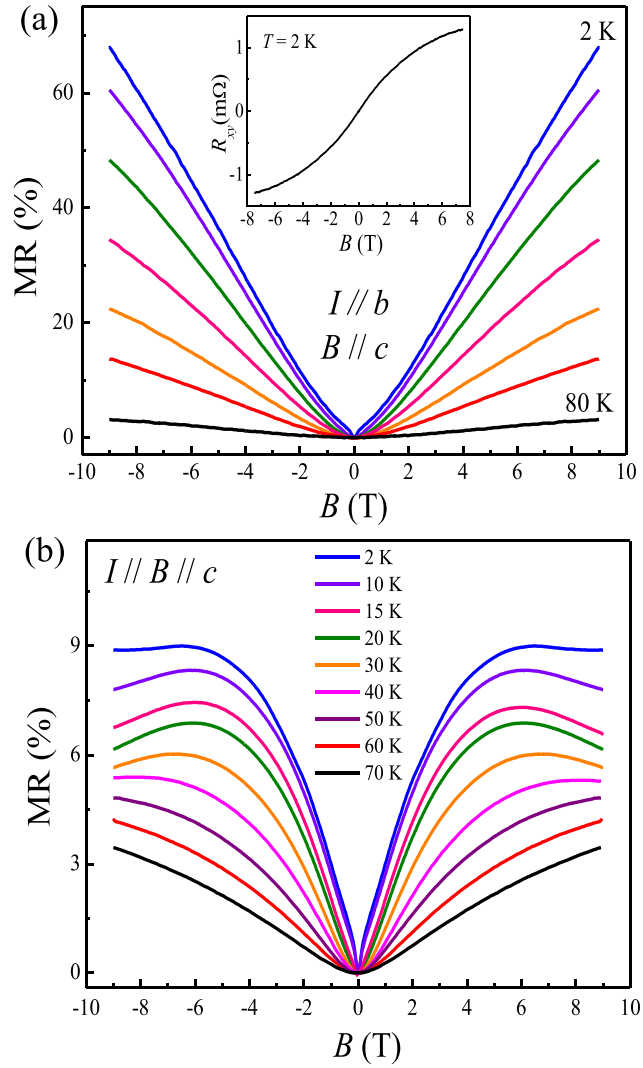

FIG. 6. Magnetic field-dependent (a) ρ_b and (b) ρ_c of γ-Mo_4O_{11} at different temperatures. The inset of (a) shows the Hall resistance at $T = 2$ K.

summarized in Fig. 8(a) and show two fundamental frequencies centered at $f_\alpha = 30$ T and $f_\beta = 131$ T with the second harmonic frequency 2β, respectively.

It is well known that the carrier density can be expressed as $n_{2D} = \upsilon_v \upsilon_s ef/h$ in 2D systems, where f is the frequency, h is the Planck constant, e is the free electron charge, and υ_v and υ_s are the valley and spin degeneracy. According to this formula, we calculate the carrier densities of the two major frequencies with $n_a = 1.54 \times 10^{16}\mathrm{m}^{-2}$ and $n_\beta = 6.18 \times 10^{16}\,\mathrm{m}^{-2}$. In addition, based on the classical Lifshitz-Kosevich theory, $\Delta\rho$ is written as the formula of $\Delta\rho/\rho_0 \propto R_T R_D \cos(2\pi f/B)$, where $R_D = \exp(-\alpha T_D m^*/B)$ and $R_T = \alpha T m^*/B\sinh(\alpha T m^*/B)$ are the Dingle damping and thermal damping factors, $\alpha = 2\pi^2 k_B m_e/(e\hbar) \sim 14.69$ T/K, m^* and T_D are the effective mass and Dingle temperature, and m_e and k_B are the free-electron mass and Boltzmann constant, respectively [35,36]. Therefore, we can further obtain the effective mass of $m_\alpha = 0.34\,m_e$ and $m_\beta = 0.27\,m_e$. The fitting effective mass values are shown in Fig. 8(b). Generally, the new oscillation frequency found in the high-field state suggests the presence of new Brillouin zones in the reciprocal space. According to the Onsager relation $S = 4\pi^2 ef/h$, the FS sizes S can be evaluated for γ-Mo_4O_{11}, which are shown as follows: $S_\alpha/S_{BZ} = 0.28\%$ and $S_\beta/S_{BZ} = 1.15\%$. To our knowledge, there are two plausible mechanisms for the quantum oscillations of γ-Mo_4O_{11} in the high-field state. One is the remaining FS pockets after the CDW transition, and another is the field-induced oscillations. Since the nonlinear transport property related to the number of CDW electrons is only observed in γ-Mo_4O_{11}, we thus argue that the normal electrons and remaining FS sizes of γ-Mo_4O_{11} in the CDW state should be less than that in η-Mo_4O_{11} (~0.2%). We further map out the approximate hole and electron pockets of γ-Mo_4O_{11} in zero field with an extremely small size (<0.2%), as shown in Fig. 8(c). Thus, the high-field oscillations of γ-Mo_4O_{11} may not be caused by the remaining FSs. In this regard, these new oscillations of γ-Mo_4O_{11} observed > 15 T are highly reminiscent of the rapid oscillations of η-Mo_4O_{11} by magnetic breakdown in a strong field [19]. Indeed, the field-

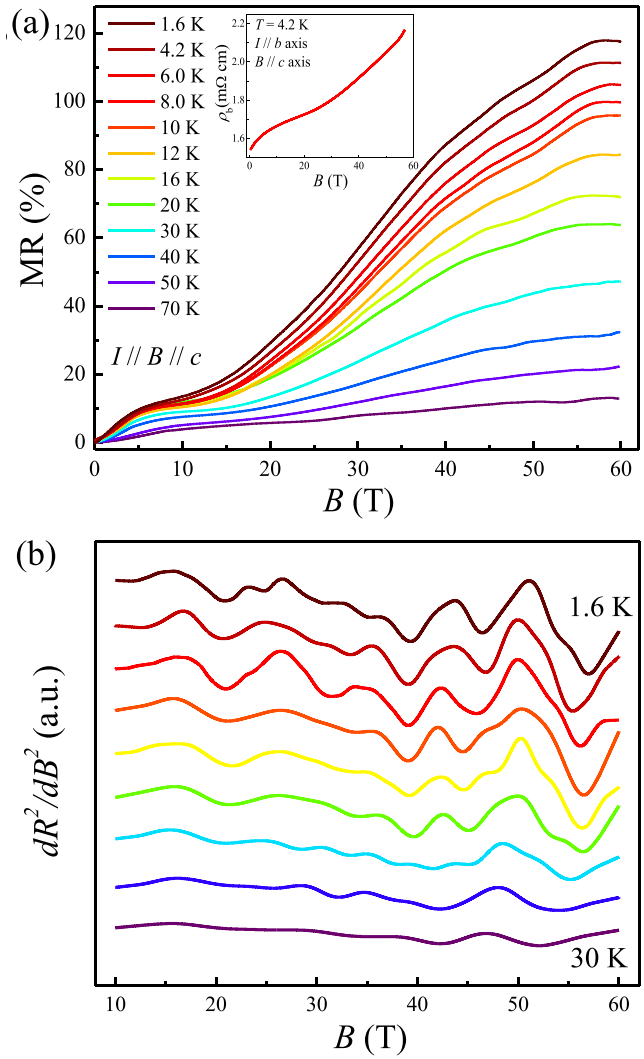

FIG. 7. (a) Magnetic field-dependent ρ_c of γ-Mo_4O_{11} from 1.6 to 70 K in fields up to 60 T. The inset shows the magnetic field-dependent ρ_b measured at 4.2 K. (b) The second derivative curves of ρ_c as a function of B. The curves have been shifted vertically for clarity.

induced oscillations associated with a magnetic breakdown between different pockets were reported in many organic superconductors and CDW materials [3,5,37–41]. The magnetic breakdown relates to the coupling of different orbits, giving rise to a new oscillation with a new frequency. Accordingly, it is reasonable to consider that the high-field quantum oscillations of γ-Mo_4O_{11} and η-Mo_4O_{11} possess a same origin. This exactly is the field-induced reconstructed FSs driven by a magnetic breakdown. On the other hand, the Q2D FS picture of γ-Mo_4O_{11} in the high-field state can be mapped out based on the calculated FS sizes via the Onsager relation. Figure 8(d) presents the approximate FS picture in the high-field state. The hole and electron pockets occupy $S_\alpha/S_{BZ} = 0.28\%$ and $S_\beta/S_{BZ} = 1.15\%$, respectively, as shown in Fig. 8(d). Note that the in-plane MR of γ-Mo_4O_{11} was also measured in a pulsed field, and the result is displayed in the inset of Fig. 7(a). However, the in-plane MR of γ-Mo_4O_{11} increases monotonically with increasing field without any oscillation character.

A summary of this part: we successfully conducted magnetotransport experiments for γ-Mo_4O_{11} in DC and pulsed fields. Well below T_{CDW}, a nonlinear transport behavior associated with the sliding of the CDW electrons is revealed in such a Q2D system. In fields up to 60 T, the field-induced quantum oscillations were discovered in the interlayer MR, which is reminiscent of the FS reconstruction of η-Mo_4O_{11} by a magnetic breakdown.

C. A comparison with η-Mo_4O_{11}

In addition to the similarities highlighted above, such as the crystal structure, FS structure in the normal phase, and the high-field oscillations, there are also some notable differences between γ-Mo_4O_{11} and η-Mo_4O_{11}. First, the CDW transition of η-Mo_4O_{11} induces two upturns in ρ_b at $T_{CDW1} = 105$ K and $T_{CDW2} = 30$ K, which are shown in the inset of Fig. 2. Note that the second CDW transition is only found for η-Mo_4O_{11}, which implies that the first CDW gap opening process should be complete at $T > 30$ K. On the other hand, the upturns in η-Mo_4O_{11} are very abrupt, and the corresponding CDW transition temperatures can be well defined, but in γ-Mo_4O_{11}, the upturn is rather flexible. The observed difference of the CDW transition indicates that their corresponding amplitude of the CDW modulation is distinguishing in these two compounds.

We now turn to the experimental evidence on the temperature-dependent susceptibility of η-Mo_4O_{11}. The susceptibility curves shown in Fig. 3(b) display an obvious phase transition at 105 K for both the $B//c$ axis and the $B//ab$ plane. This is analogous with the results observed in γ-Mo_4O_{11}, indicative of the similarity of the two systems in the normal phase. When $T < T_{CDW1}$, the susceptibility of η-Mo_4O_{11} decreases sharply and shows another anomaly at 30 K, consistent with the second CDW transition found in resistivity. For both the $B//c$ axis and the $B//ab$ plane, the susceptibility of η-Mo_4O_{11} shows a pronounced transition at the onset of CDW, which suggests that the CDW modulations are strong and identical along the ab plane and the c axis. However, like the difference in the upturn of resistivity, the susceptibility transitions of η-Mo_4O_{11} are more robust than that of γ-Mo_4O_{11}. This further supports that the CDW modulation of γ-Mo_4O_{11} is discontinuous and different from that of η-Mo_4O_{11} in which the CDW transition is abrupt.

The temperature-dependent specific heat C_p of η-Mo_4O_{11} (black line), shown in Fig. 4, uncovers another distinct difference between the two systems. A slight specific heat anomaly is detected between 102 and 106 K for η-Mo_4O_{11}, which agrees with the CDW transition in resistivity and susceptibility. The existence of the specific heat anomaly for η-Mo_4O_{11} indicates that the CDW modulation is relatively stronger, like the observation in $K_{0.9}Mo_6O_{17}$ [28]. The inset of Fig. 4 shows the corresponding C_p/T result of η-Mo_4O_{11} for clarity. By contrast, the CDW transition of γ-Mo_4O_{11} cannot be detected by specific heat measurement due to a weak lattice modulation. Moreover, as shown in Fig. 5(b), the I-V curves of η-Mo_4O_{11} show a good linear relation in applied current up to 100 mA. It means that the dominate carriers involved in the transport for η-Mo_4O_{11} are the normal electrons rather than the CDW electrons. By contrast, a nonlinear I-V relation is found in γ-Mo_4O_{11} because the CDW gap is nearly fully opened, and all the residual electrons contribute to the CDW transport.

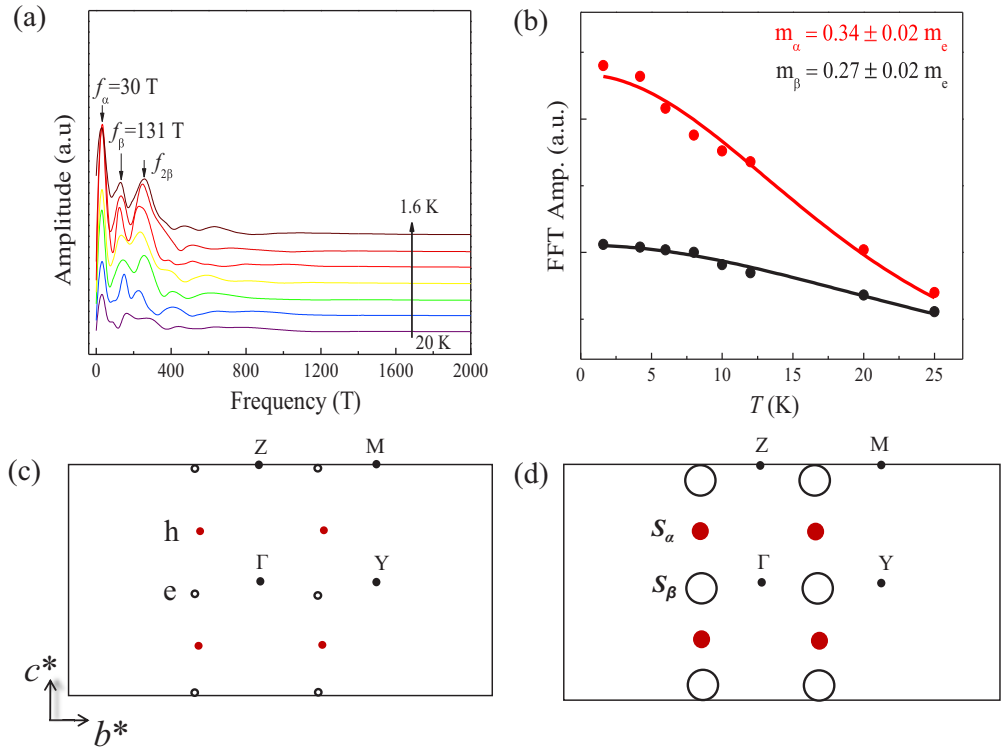

FIG. 8. (a) The fast Fourier transform (FFT) spectra of the high-field oscillations in the temperature range of $1.6 < T < 20$ K. (b) The Lifshitz-Kosevich fitting for f_α and f_β. (c) The approximate Fermi surface (FS) sizes for γ-Mo_4O_{11} in zero field. (d) The calculated FS sizes for γ-Mo_4O_{11} in the high-field state.

In recent high-field MR experiments for η-Mo_4O_{11}, a sharp increase of ρ_c and rapid oscillations at $B > 15$ T were also observed [19]. However, the observed SdH oscillations of η-Mo_4O_{11} are more remarkable than that of γ-Mo_4O_{11}. It can be seen even in the raw data of Fig. 7(a) that the oscillation frequency in γ-Mo_4O_{11} is much lower than that in η-Mo_4O_{11}, which clearly suggests that these two phases of Mo_4O_{11} possess different band structure at low temperatures. The high-field MR of η-Mo_4O_{11} resolved the highest frequency of 2640 T above 45 T, which cannot be detected for γ-Mo_4O_{11} in the same field range. The calculated FS sizes in the high-field state of γ-Mo_4O_{11} are much smaller than that of η-Mo_4O_{11} ($S/S_{BZ} = 23.5\%$), which is nearly identical to FS sizes ($\sim$25%) in the normal phase ($T > T_{CDW}$). In this regard, the scenario is also reminiscent of the other two Q2D sister purple bronzes $K_{0.9}Mo_6O_{17}$ and $Na_{0.9}Mo_6O_{17}$, in which the highest frequency $\sim$2800 T was also uncovered due to a magnetic breakdown effect in recent ultrahigh-field experiments up to 80 T [3]. However, the critical field required for the highest breakdown frequency is 50 T in $Na_{0.9}Mo_6O_{17}$, while it is 70 T in $K_{0.9}Mo_6O_{17}$, owing to a larger CDW gap [3,42,43]. Moreover, the resolved frequency of γ-Mo_4O_{11} up to 60 T is exactly in the same order with the frequency of η-Mo_4O_{11} revealed for $15\ \text{T} < B < 45$ T [19]. Consequently, it is reasonable to propose that γ-Mo_4O_{11} has a relatively larger CDW gap and requires a higher critical field to achieve its highest breakdown frequency in experiment. As we know, the only difference between the two compounds is that η-Mo_4O_{11} is monoclinic, and γ-Mo_4O_{11} has an orthorhombic structure. However, the calculated FS sizes of η-Mo_4O_{11} are much larger than that of γ-Mo_4O_{11} at low temperatures. Accordingly, the main influence caused by the different crystal structures can be understood as the temperature-dependent CDW gaps: the first opening of the gap appears to be complete at $T > 30$ K in η-Mo_4O_{11}, and the FSs undergo a second transition. In γ-Mo_4O_{11}, the gaps continue to open until the lowest temperature. However, to confirm the FS structure of γ-Mo_4O_{11} in the low-temperature CDW state, further detailed evidence, such as transport experiments under higher fields, angle-resolved photoemission spectroscopy measurements, and density functional theory calculations, is desired in future studies.

IV. CONCLUSIONS

In summary, we report a comprehensive study of the sample synthesis, magnetic susceptibility, specific heat, and transport properties in the Q2D CDW compound γ-Mo_4O_{11}. These results establish that γ-Mo_4O_{11} belongs to a Q2D system and undergoes a CDW transition at $T_{CDW} \sim 96$ K. Well below T_{CDW}, a nonlinear current-voltage characteristic relation was discovered in such a Q2D system. The interlayer MR up to 60 T exhibits field-induced quantum oscillations in the CDW state, which are reminiscent of a FS reconstruction of η-Mo_4O_{11} by a magnetic breakdown in a strong field. A comparative study on the two systems suggests that the CDW transition in γ-Mo_4O_{11} is relatively flexible, while the CDW transition in η-Mo_4O_{11} is abrupt. Finally, measurements of the high-field MR also support that γ-Mo_4O_{11} has a nearly fully opened CDW gap and thus a higher breakdown field than that of η-Mo_4O_{11}.

ACKNOWLEDGMENTS

This paper was supported by the National Natural Science Foundation of China (Grants No. U1832214, No. 12004122, No. 12074135, No. 11974061, and No. 12074291) and the Fundamental Research Funds for the Central Universities (Grants No. 2018KFYXKJC005 and No. 2019kfyXJJ009).

[1] M. H. Whangbo, E. Canadell, P. Foury, and J. P. Pouget, Science **252**, 96 (1991).

[2] J. F. Wang, M. Yang, L. Li, M. Sasaki, A. Ohnishi, M. Kitaura, K. S. Kim, and H. J. Kim, Phys. Rev. B **89**, 035137 (2014).

[3] H. P. Zhu, M. Yang, J. Z. Ke, H. K. Zuo, T. Peng, J. F. Wang, Y. Liu, X. F. Xu, Y. Kohama, and K. Kindo, Phys. Rev. B **102**, 235164 (2020).

[4] J. Dumas, H. Guyot, H. Balaska, J. Marcus, D. Vignolles, I. Sheikin, A. Audouard, L. Brossard, and C. Schlenker, Physica B **346**, 314 (2004).

[5] X. H. Qin, J. Shi, H. Y. Gong, M. L. Tian, J. Y. Wei, H. Chen, and D. C. Tian, Phys. Rev. B **53**, 15538 (1996).

[6] N. Lera and J. V. Alvarez, Phys. Rev. B **92**, 174523 (2015).

[7] J. F. Mercure, A. F. Bangura, X. F. Xu, N. Wakeham, A. Carrington, P. Walmsley, M. Greenblatt, and N. E. Hussey, Phys. Rev. Lett. **108**, 187003 (2012).

[8] F. Wang, J. V. Alvarez, S. K. Mo, J. W. Allen, G. H. Gweon, J. He, R. Jin, D. Mandrus, and H. Höchst, Phys. Rev. Lett. **96**, 196403 (2005).

[9] X. F. Xu, A. F. Bangura, J. G. Analytis, J. D. Fletcher, M. M. J. French, N. Shannon, J. He, S. Zhang, D. Mandrus, R. Jin, and N. E. Hussey, Phys. Rev. Lett. **102**, 206602 (2009).

[10] M. Sasaki, N. Miyajima, H. Negishi, W. X. Gao, M. Inoue, H. Kadomatsu, G. Machel, H. Nojiri, and M. Matokawa, J. Phys. Soc. Jpn. **68**, 539 (1999).

[11] M. Inoue, S. Ohara, S. Horisaka, M. Koyano, and H. Negishi, Phys. Status Solidi B **148**, 659 (1988).

[12] M. S. D. Luz, A. D. Campos, B. D. White, and J. J. Neumeier, Phys. Rev. B **79**, 233106 (2009).

[13] M. Sasaki, G. X. Tai, S. Tamura, and M. Inoue, Phys. Rev. B **47**, 6216 (1993).

[14] S. Hill, S. Uji, M. Takashita, C. Terakura, T. Terashima, H. Aoki, J. S. Brooks, Z. Fisk, and J. Sarrao, Phys. Rev. B **58**, 10778 (1998).

[15] M. Sasaki, N. Miyajima, H. Negishi, K. Suga, Y. Narumi, and K. Kindo, Physica B **298**, 520 (2001).

[16] K. I. Suga, A. Ohnishi, M. Koyano, M. Sasaki, and K. Kindo, J. Phys. Soc. Jpn. **77**, 074605 (2008).

[17] S. Hill, S. Valfells, S. Uji, J. S. Brooks, G. J. Athas, P. S. Sandhu, J. Sarrao, Z. Fisk, J. Geoette, H. Aoki, and T. Terashima, Phys. Rev. B **55**, 2018 (1997).

[18] Z. Y. Liu, P. F. Shan, K. Y. Chen, M. Marshall, S. Zhang, T. Yong, H. S. Deng, X. Yin, Y. Ding, H. M. Weng, Y. Uwatoko, P. Dera, W. W. Xie, Y. Sui, and J.-G. Cheng, Phys. Rev. B **104**, 024105 (2021).

[19] J. Z. Ke, M. Yang, H. P. Zhu, C. B. Liu, C. Dong, W. X. Liu, M. Y. Shi, and J. F. Wang, Phys. Rev. B **102**, 245135 (2020).

[20] K. Y. Chen, N. N. Wang, Q. W. Yin, Y. H. Gu, K. Jiang, Z. J. Tu, C. S. Gong, Y. Uwatoko, J. P. Sun, H. C. Lei, J. P. Hu, and J. G. Cheng, Phys. Rev. Lett. **126**, 247001 (2021).

[21] B. R. Ortiz, S. M. L. Teicher, Y. Hu, J. L. Zuo, P. M. Sarte, E. C. Schueller, A. M. M. Abeykoon, M. J. Krogstad, S. Rosenkranz, R. Osborn, R. Seshadri, L. Balent, J. He, and S. D. Wilson, Phys. Rev. Lett. **125**, 247002 (2020).

[22] J. Z. Ke, M. Yang, H. K. Zuo, H. P. Zhu, C. B. Liu, R. Chen, C. Dong, W. X. Liu, M. Y. Shi, and J. F. Wang, J. Alloys Compd. **835**, 155417 (2020).

[23] H. K. Fun, P. Yang, M. Sasaki, M. Inoue, and H. Kadomatsu, Powder Diffr. **14**, 284 (1999).

[24] M. Koyano, S. Ohara, H. Negishi, M. Sasaki, M. Nomura, and H. Fujiwara, Phys. Status Solidi B **147**, 559 (1988).

[25] R. Buder, J. Devenyi, J. Dumas, J. Marcus, J. Mercier, C. Schlenker, and H. Vincent, J. Phys. Lett. **43**, 59 (1982).

[26] M. L. Tian, S. Yue, J. Shi, S. Y. Li, and Y. H. Zhang, J. Phys.: Condens. Matter **13**, 311 (2001).

[27] R. S. Kwok and S. E. Brown, Phys. Rev. Lett. **63**, 895 (1989).

[28] C. Escribe-Filippini, K. Konate, J. Marcus, C. Schlenker, R. Almairac, R. Ayroles, and C. Roucau, Philos. Mag. B **50**, 321 (1984).

[29] J. Dumas, C. Schlenker, J. Marcus, and R. Buder, Phys. Rev. Lett. **50**, 757 (1983).

[30] D. H. Li, R. Xiong, J. F. Wang, C. Z. Li, D. Yin, F. Yi, W. F. Tang, and J. Shi, Chin. Phys. Lett. **22**, 1210 (2005).

[31] C. A. Balseiro and L. M. Falicov, Phys. Rev. B **34**, 863 (1985).

[32] D. Graf, J. S. Brooks, E. S. Choi, S. Uji, J. C. Dias, M. Almeida, and M. Matos, Phys. Rev. B **69**, 125113 (2004).

[33] J. S. Qualls, L. Balicas, J. S. Brooks, N. Harrison, L. K. Montgomery, and M. Tokumoto, Phys. Rev. B **62**, 10008 (2000).

[34] E. Canadell, M. H. Whangbo, C. Schlenker, and C. Escribe-Filipppini, Inorg. Chem. **28**, 1466 (1989).

[35] D. Shoenberg, *Magnetic Oscillations in Metals* (Cambridge University Press, Cambridge, 1984).

[36] N. W. Ashcroft and N. D. Mermin, *Solid State Physics* (Holt, Rinehart and Winston, New York, 1976).

[37] P. Walmsley, S. Aeschlimann, J. A. W. Straquadine, P. Giraldo-Gallo, S. C. Riggs, M. K. Chan, R. D. Mcdonald, and I. R. Fisher, Phys. Rev. B **102**, 045150 (2020).

[38] S. K. Lewin and J. G. Analytis, Phys. Rev. B **92**, 195130 (2015).

[39] S. E. Sebastian, N. Harrison, R. X. Liang, D. A. Bonn, W. N. Hardy, C. H. Mielke, and G. G. Lonzarich, Phys. Rev. Lett. **108**, 196403 (2012).

[40] T. Helm, M. V. Kartsovnik, I. Sheikin, M. Bartkowiak, F. W. Fabris, N. Bittner, W. Biberacher, M. Lambacher, A. Erb, J. Wosnitza, and R. Gross, Phys. Rev. Lett. **105**, 247002 (2010).

[41] V. M. Gvozdikov, A. G. M. Jansen, D. A. Pesin, I. D. Vagner, and P. Wyder, Phys. Rev. B **70**, 245114 (2004).

[42] P. A. Glans, T. Learmonth, K. E. Smith, T. Valla, P. D. Johnson, S. L. Hulbert, W. McCarroll, and M. Greenblatt, Phys. Rev. B **72**, 035115 (2005).

[43] L. Su, C. H. Hsu, H. Lin, and V. M. Pereira, Phys. Rev. Lett. **118**, 257601 (2017).